

Leszek Chybowski

ORCID ID: 0000-0003-0245-3946

Damian Kazienko

ORCID ID: 0000-0002-7331-7960

Maritime University of Szczecin, Poland

INTRODUCTION

A ship's internal combustion engine is usually equipped with diagnostic subsystems that are used to assess the performance of the engine during operation, as well as to detect engine malfunctions and to locate any faults as per the adopted operating strategy (Piasecki et al., 2017; Chybowski, 2018; Chybowski, Gawdzińska and Souchkov, 2018; Chybowski, Gawdzińska and Laskowski, 2019; Kazienko, 2019; Bejger and Piasecki, 2020). Depending on the purpose and design of the machine, different diagnostic methods can be used (Kluj, 2000; Quan, W., Wei, J., Zhao, YW., Sun, LH., Bianl, 2011; Borkowski, T. Kowalak, P. Myśków, 2012; Ulewicz and Mazur, 2013; Bonisławski et al., 2019; Dunaj, Dolata and Berczyński, 2019; Dunaj, Marchelek and Chodźko, 2019; Ulewicz et al., 2019). For diesel engines that are equipped with indicator cocks, the graphs of the combustion pressure can be analyzed to provide this data (Bueno, Velásquez and Milanez, 2009; Chybowski, 2019). In a ship's engine rooms, there are so-called parametric diagnostic methods that are widely used and which consist of measuring the engine's working parameters, such as temperature, pressure, flow, etc. (Korczewski, 2015; Chybowski and Kazienko, 2019). The above-mentioned methods are complemented by tools that use the dissipation of energy that is associated with residual processes that occur during operation of the machine (Bejger, Chybowski and Gawdzińska, 2018). The methods in the last group include vibration diagnostics (Bejger and Drzewieniecki, 2019, 2020) and thermovision methods (Krystosik-Gromadzińska, 2019).

This article presents the results of a study related to the development of an original system to diagnose the combustion process in internal combustion engines (Kazienko and Chybowski, 2020). The engine is analyzed following the measurement and analysis of changes in the engine's instantaneous speed. Thus, this method is of interest for authors researching parametric diagnostics contrary to verification methods (Chybowski et al., 2020). This system allows an

engine to be monitored in both steady and transient states by detecting and locating any disturbances; This system allows an engine to be monitored in both steady and transient states by detecting and locating any non-uniformity in the engine operation, in particular, a misfire in one of the cylinders.

There have been many studies concerning the use of the change in the instantaneous speed in the assessment of the health of internal combustion engines (Margaronis, 1992; Yang et al., 2001; Desbazeille et al., 2010; Li et al., 2012; Tagliatela et al., 2013; Dereszewski, 2016; Biočanin and Biočanin, 2017; Wang et al., 2019). However, these studies were not usually geared towards implementing their results in the operation of a ship. This may be the result of the lack of a universal algorithm for analyzing changes in an engine's instantaneous speed, which could then be applied to different types of engines. Each installation of such a system for a new engine requires pattern acquisition and the inclusion of data on the engine's operating conditions and characteristics in the algorithm. In the authors' previous paper (Kazienko and Chybowski, 2020), a promising algorithm was presented which does not require a lot of work during the system's start-up.

The instantaneous speed of an engine can be successfully used as a diagnostic parameter in assessing the health of engines equipped with other diagnostic systems, e.g. combustion pressure measurement (Caputo et al., 2018). Changes of engine speed are reflecting changes of torque (Nozdrzykowski, 2005, 2016; Nozdrzykowski and Bejger, 2013). In those cases, the proposed system will act as a complementary tool. In addition, the system can be used as an essential diagnostic tool for engines with no indicator cocks. Low and medium-power ship, traction and stationary engines are not usually fitted with indicator cock valves or advanced diagnostic systems, which makes monitoring these engines very difficult. These engines include machines made by Detroit Diesel, Caterpillar, Daimler Chrysler, John Deere, Scania, Volvo, etc.

The experiments that have been previously carried out by the authors on a Buckau-Wolf R8VD-136 engine driving a shipborne fixed-pitch propeller and a Sulzer 5 BAH 22 engine driving an alternating current generator have confirmed the correct operation of the system as well as its flawless detection of a misfiring cylinder. Figure 1 illustrates the difference between the graphs of the instantaneous speed of a fully operative engine and the instantaneous speed of a Buckau-Wolf R8VD-136 engine in which combustion was lost in cylinder 1.

In developing this system, it was important to properly select and use the quantitative indicators of the changes in the instantaneous engine speed obtained during operation. The change in the instantaneous engine speed $n(\text{rpm})$ may be a function of the crankshaft's angle of rotation $\alpha(^{\circ}\text{CA})$, described by equal numeric indicators. One of the simplest indicators is the maximum difference in the rotational speed Δn_{max} during an engine's full operating cycle.

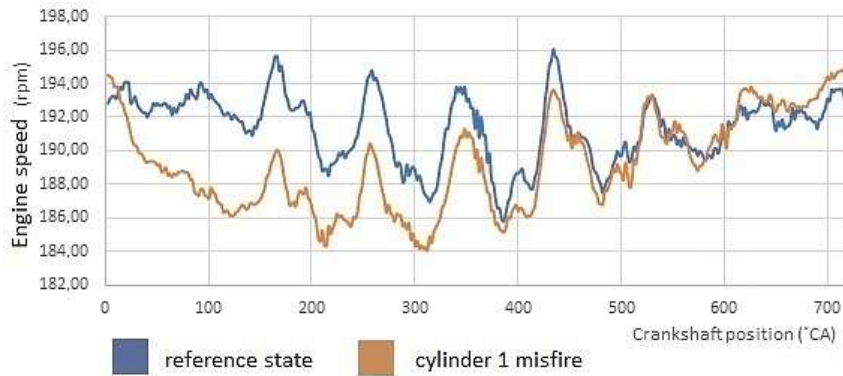


Fig. 1 The instantaneous speed difference of a Buckau-Wolf R8VD-136 engine observed for the loss of combustion in one of the cylinders (Kazienko and Chybowski, 2020)

This quantity can be expressed by the following equation:

$$\Delta n(\alpha)_{max} = n(\alpha)_{max} - n(\alpha)_{min} \quad (\text{rpm}) \quad (1)$$

where:

$n(\alpha)_{max}$ – highest angular speed during one operating cycle of the engine,

$n(\alpha)_{min}$ – lowest angular speed during one operating cycle of the engine,

α – angle of crankshaft rotation $\alpha \in < 0, \frac{360}{\tau}>$,

τ – number of ignition points in a cylinder for one full rotation of the crankshaft:

$\tau = 1$ for two-stroke engines, $\tau = 0.5$ for four-stroke engines.

A widely used indicator for describing the variation in engine speed during one full operating cycle is the speed uniformity $\delta(\%)$, which may be expressed as follows:

$$\delta = 200 \frac{n(\alpha)_{max} - n(\alpha)_{min}}{n(\alpha)_{max} + n(\alpha)_{min}} \quad (\%) \quad (2)$$

This indicator is the ratio between the maximum difference in instantaneous speed during an engine's full operating cycle and the average of the maximum and minimum speeds during one engine cycle.

The analyses allowed the authors to come to the conclusion that an additional speed change indicator, which could be used to assess an engine's health, is what the authors called the differential speed area factor D_{SAF} (deg^2/s), which represents the change in the area under the curve of the momentary speed $n = f(\alpha)$ between the operational situation F_{op} and the reference curve F_{ref} , as described by the following equation:

$$D_{SAF} = F_{op} - F_{ref} \quad \left(\frac{\text{deg}^2}{\text{s}} \right) \quad (3)$$

The area under the speed change curve can be described by the formula:

$$F = 6 \int_{\alpha=0}^{\alpha=\frac{360}{\tau}} n(\alpha) d\alpha \quad \left(\frac{\text{deg}^2}{\text{s}} \right) \quad (4)$$

The authors' study has shown that a decrease in the area under the speed change curve may indicate disturbances in the engine's combustion. In addition, the relationship between the change of the surface area and the angular position can be used to identify the cylinder in which combustion has been lost. Visualization of this issue using polar coordinates has been presented in an earlier paper by the authors (Kazienko and Chybowski, 2020).

This article presents the values of the aforementioned quantitative indicators, for different engine loads and different operating states, obtained under experimental conditions. For each different set speed of the engine, the instantaneous speed was measured for the reference state as well as for the states where one of the cylinders was out of operation. Cylinders 1-8 were consecutively put out of operation so that only one was out at a time, and all the other cylinders operated normally; the indicators (1), (2) and (3) were then calculated for all of the obtained graphs.

MATERIALS AND METHODS

The tests were performed on a Buckau-Wolf R8VD-136 ship's engine (Chybowski *et al.*, 2020) as shown in Figure 2.



Fig. 2 A view of the VEB SKL – Buckau-Wolf R8VD-136 Engine

Source: (Nozdrzykowski, Chybowski and Dorobczyński, 2020)

It is the main propulsion engine of a ship that actuates a fixed-pitch propeller; the basic specification of the engine is listed in Table 1.

Table 1 The basic technical and operational parameters of the Buckau-Wolf R8VD-136 Engine

Parameter	Description	Parameter	Description
Manufacturer	VEB SKL – Magdeburg	Compression chamber volume	1.205 dm ³
Power consumption	Fixed-pitch propeller	Nominal effective power	220 kW
Type	4-stroke, naturally aspirated, trunk engine	Nominal speed	360 rpm
Dry engine weight (without flywheel)	9600 kg	Nominal mean effective pressure	0.56 MPa
Weight of flywheel	900 kg	Nominal compression pressure	3.53 MPa
Number of cylinders	8	Nominal maximum combustion pressure	5.09 MPa
Cylinder bore	240 mm	Nominal mean piston speed	4.32 m/s
Piston stroke	360 mm	Nominal specific fuel oil consumption	238 g/kWh
Cylinder's working volume	16.290 dm ³	Firing order	1-2-5-6-8-7-4-3

Source: (VEB SKL, 1960)

Figure 3 shows the elements of the measurement circuit named 'SpeedMA' by the authors. The instantaneous speed was measured using an incremental encoder, measuring the crankshaft angle, which was installed at the free end of the engine's crankshaft. The accuracy of the measurement was 1°CA (crank angle).

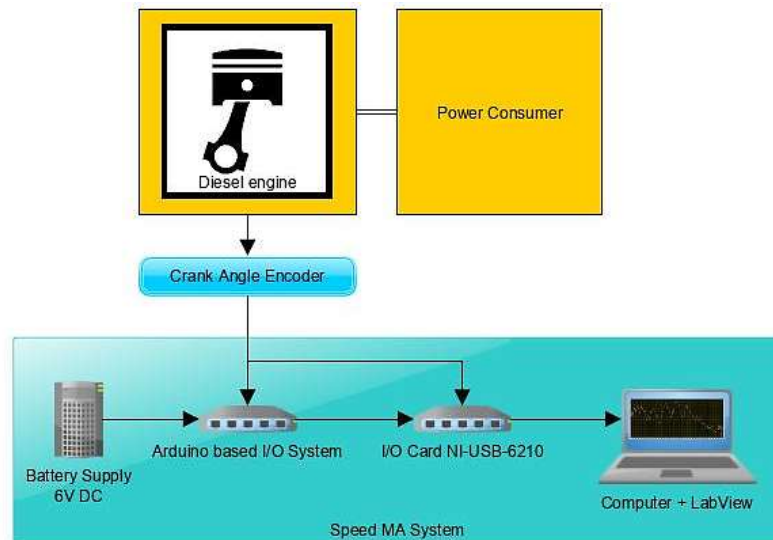


Fig. 3 Diagram of the measuring system

Source: (Kazienko and Chybowski, 2020)

Top dead center (TDC) for cylinder 1 was synchronized using a microcomputer with an Artmega 2560 system and an Arduino Industrial 101 board. The final measurement was performed by means of a National Instruments USB-6210 card. The data from the measurement card was processed by a program running on a PC using the LabView environment from National Instruments.

The screenshot in Figure 4 shows an example of the analysis of an engine's operation for a pre-set rotational speed of 220 rpm and a maximum deviation setting of 1.5%.

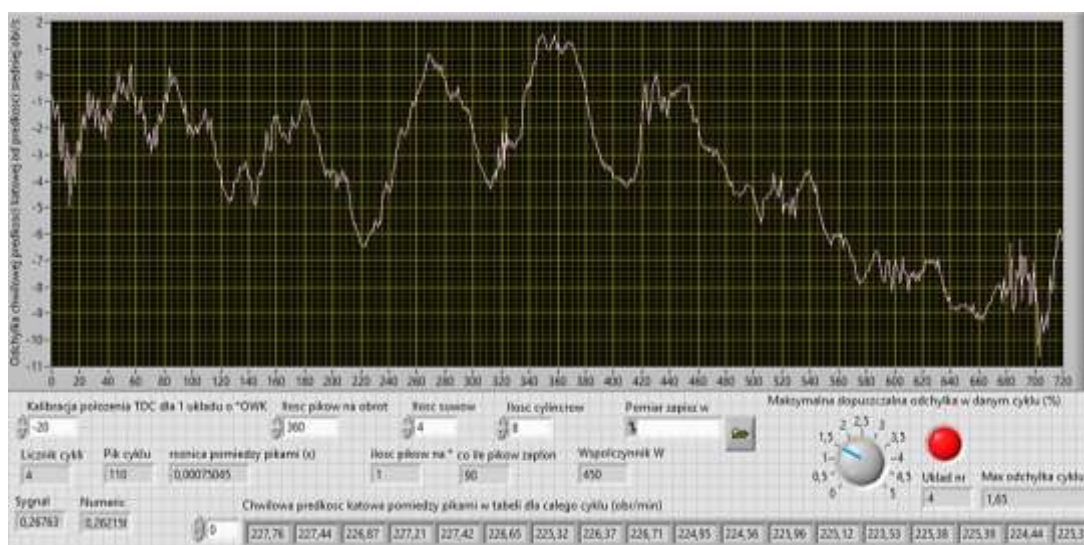


Fig. 4 Screenshot of the detection program for lack of combustion for cylinder 4

Once the fuel pump of the fourth cylinder was shut off, the change in the coefficient of the maximum deviation exceeded the set limit value, resulting in the alarm sounding.

During the experiment, the standard engine operating speeds were used; the speed then ranged from 200 to 280 rpm with an increment at 20 rpm. Cylinders were switched off by turning off the fuel pump with the use of a shut-off shaft placed on each of the injection pumps. At the same time, for each operating condition, the load indicator values were recorded. The values were read from the pointer installed on the fuel lever that controls the injection pumps via the speed governor. The indications of the instantaneous fuel charge supplied by the fuel pumps to the injectors are presented as dimensionless figures on a scale of 0-14. Table 2 shows the load indicator values for each of the speed setpoints with the engine operating under standard conditions and with one of the cylinders out of operation.

Table 2 Values of the load indicator for the analyzed operating conditions

Speed setpoint (rpm)	200	220	240	260	280
Load indicator for normal operation	3.5	4.0	4.5	5.0	5.5
Load indicator for a single cylinder misfire	3.8	4.4	5.0	5.6	6.2

Source: the authors.

Any noise or distortion in the signal was removed by means of a six-point moving average filter. The analysis used the average of the graphs of the changes in the instantaneous engine speed averaged over the five successive operating cycles. The collected measurement data then served to determine the quantitative indicators that describe the engine's condition.

RESULTS AND DISCUSSION

Figures 5-7 illustrate the changes in the selected recorded instantaneous engine speeds; Figure 5 shows the reference cycles.

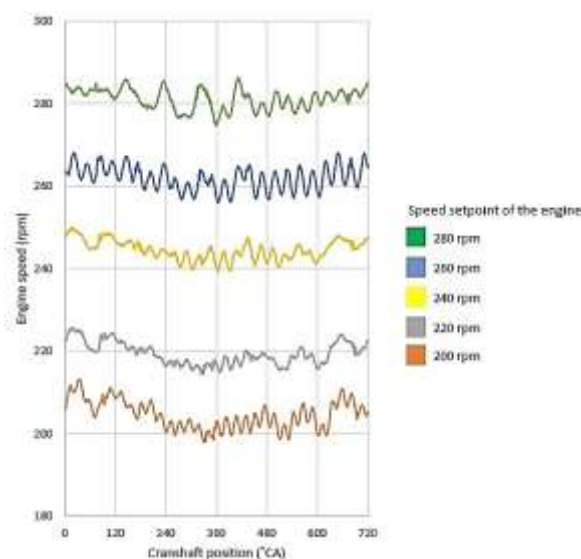


Fig. 5 Recorded graphs of the instantaneous speed change for a fully operative engine

The effect of loss of combustion in one of the cylinders for the graph of the changes in the instantaneous rotational speed of the engine is shown in Figures 6 and 7.

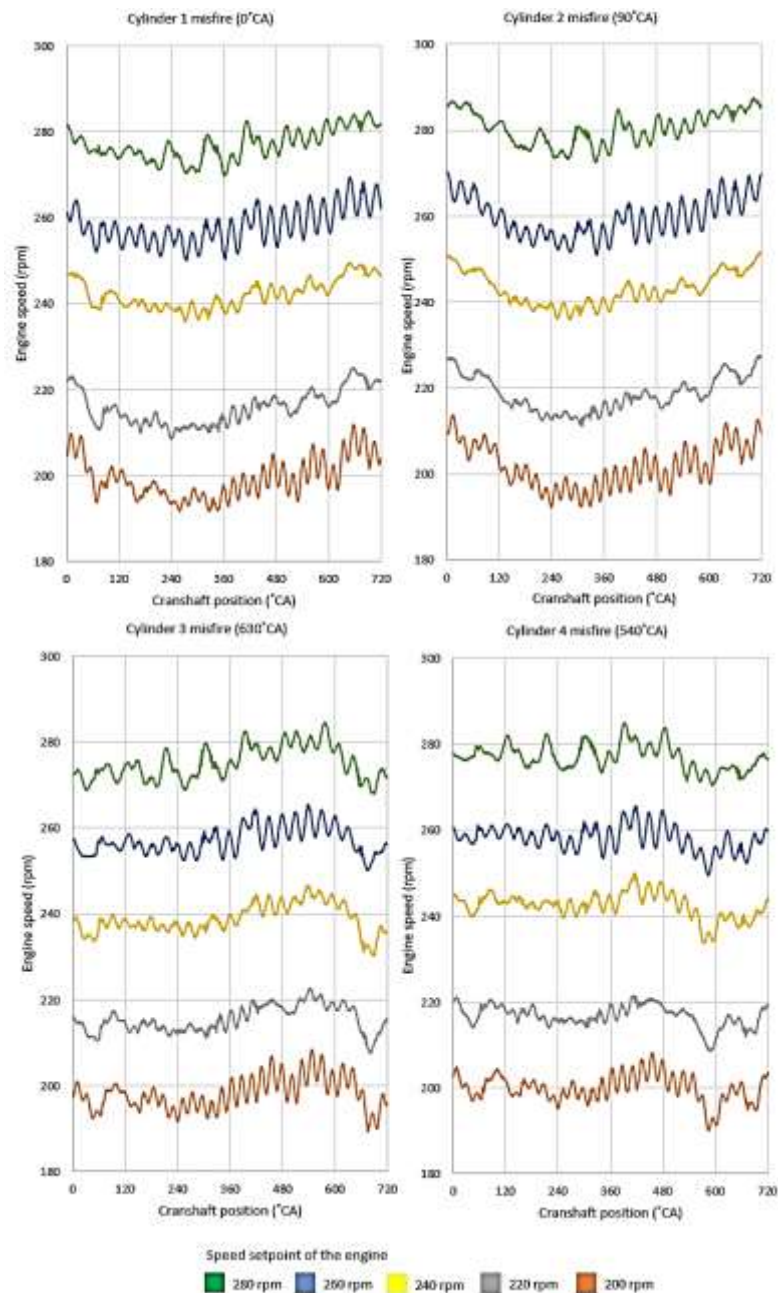


Fig. 6 Recorded graphs of the instantaneous speed change for a misfire in one of the cylinders (cylinders 1-4)

For each of the analyzed situations, there is a shared characteristic where the change in the average speed is comparable regardless of the load resulting from the speed setpoint. Shown above each of the combustion fault graphs, is the angular position of the engine's crankshaft at which ignition should occur. Immediately after the expected ignition point, which has been disabled, a decrease in the engine's rotational speed can be observed; this can be used to locate the misfiring cylinder.

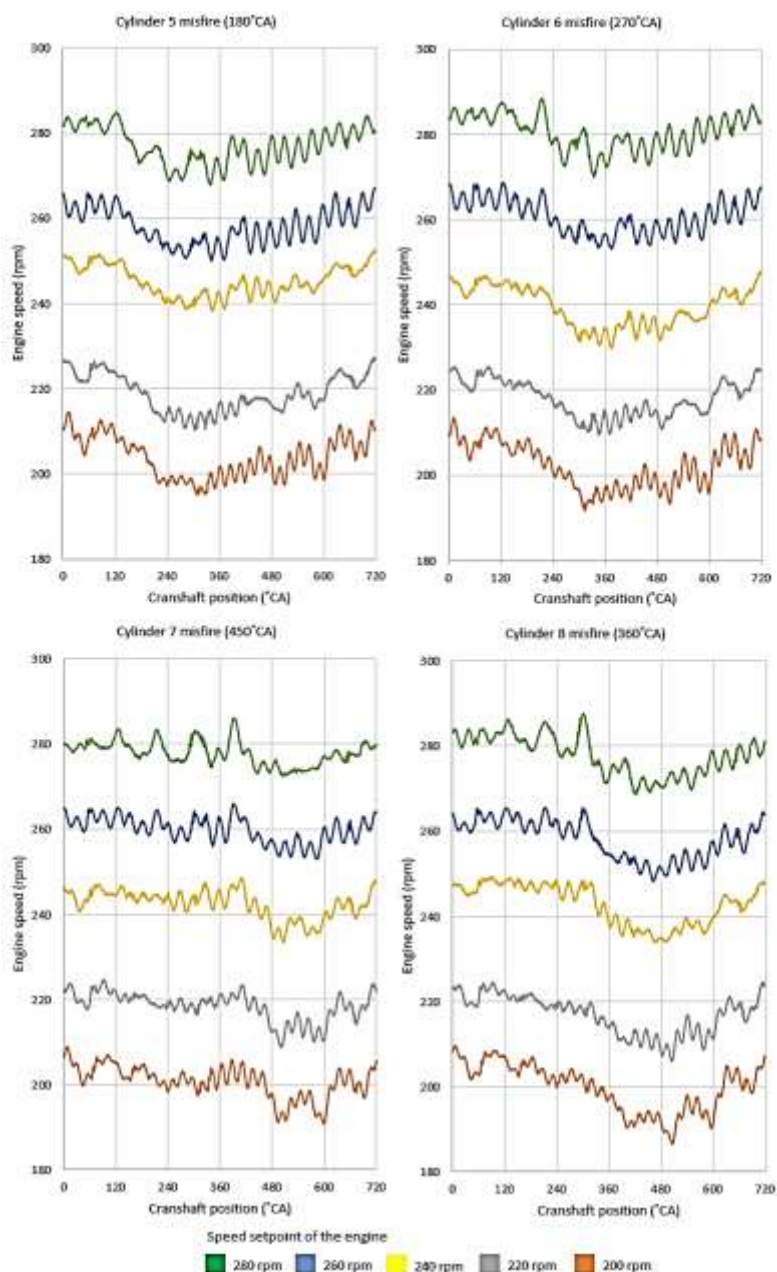


Fig. 7 Recorded graphs of the instantaneous speed change for a misfire in one of the cylinders (cylinders 5-8)

The quantitative indicators that have been presented in the introduction were then applied to the experimental data. Figure 8 shows the maximum differences in the rotational speed over the engine's full operating cycle during the experiment. When combustion in one of the cylinders does not occur, the graph then differs significantly for each load as well as for the cylinder in which the issue occurred. The values of this indicator for an engine with a misfiring cylinder range from 12.5 to 23 rpm. The nature of these changes is very complex and does not directly allow identification of the cylinder in which combustion was lost.

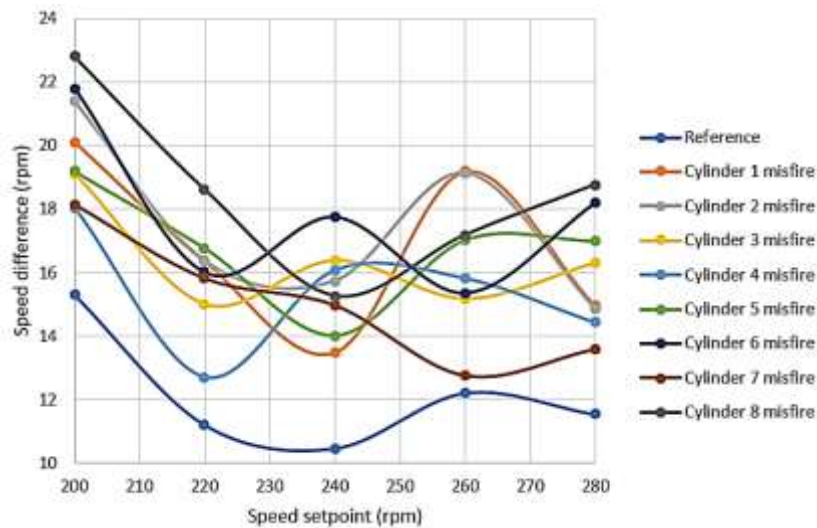


Fig. 8 The maximum differences in the rotational speed over the engine's full operating cycle obtained from the experiment

In each of the analyzed cases, the maximum difference in the speed variation is greater than in the reference graph. Hence, the maximum difference in instantaneous speed over the engine's full operating cycle is a good source of information; it does not indicate the location of the disturbance (number of the misfiring cylinder), but does indicate that the combustion process was disturbed. The values of the uniformity of the engine's speed are presented in Figure 9.

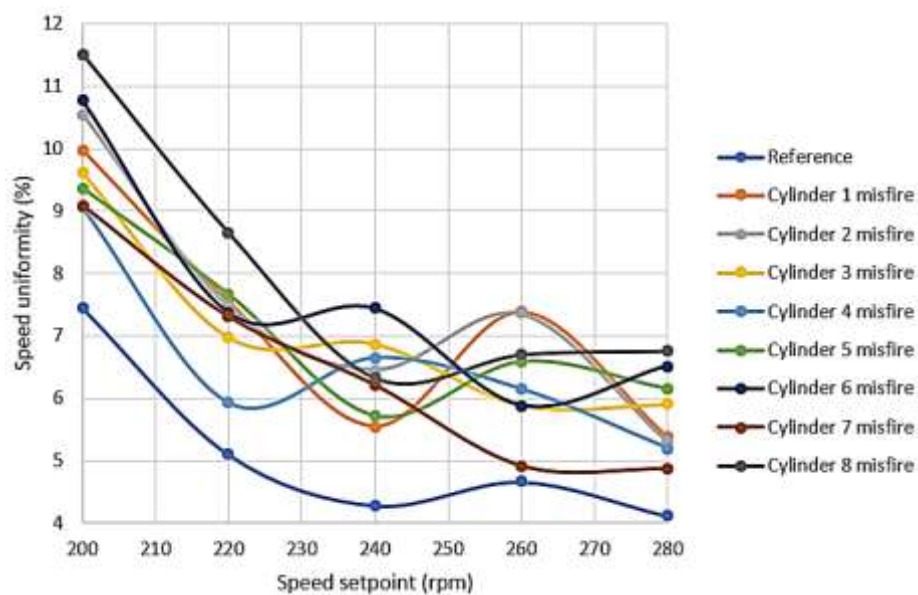


Fig. 9 Speed uniformity values obtained from the experiment

As in the case of the maximum speed differences, the graphs display very different characteristics. This indicator ranges from 5-12% for combustion loss in one of the cylinders of the engine being tested. For all of the rotational speed setpoints, the indicator's value for the reference conditions is lower than that for a misfire in one of the cylinders. When the engine is operating correctly, for a speed between 200-220 rpm, the value of δ ranges from 5-7.5%, which is due

to the low load and the speed setpoint that is close to the engine’s minimum speed. For the remainder of the range, the values of δ are smaller than 5%, which meets the requirements of the classification societies for the ship's main propulsion engines. The value of the indicator δ is able to provide information on the quality of the combustion process in the engine’s cylinders.

Figure 10 shows the values of the differential speed area factor D_{SAF} .

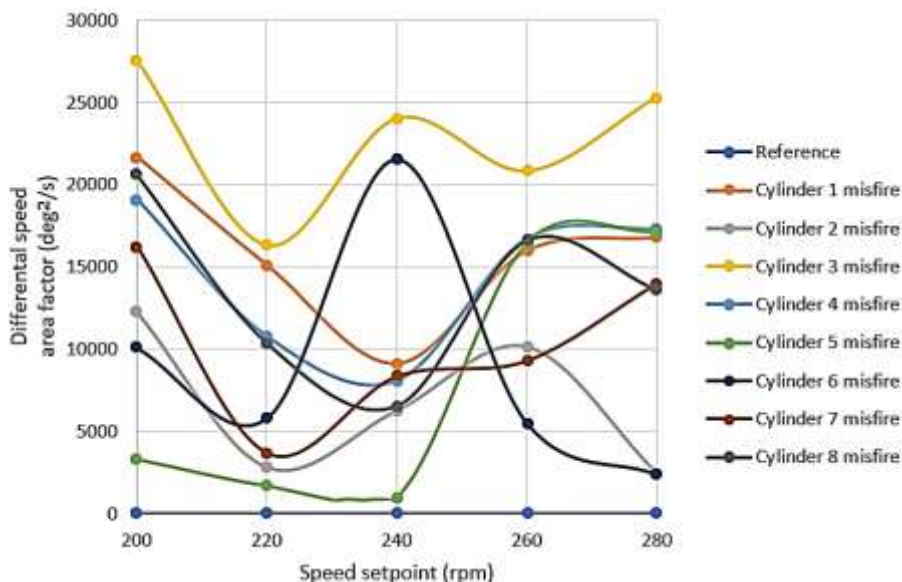


Fig. 10 Differential speed area factor values obtained in the experiment

Except for misfires on cylinders 5 and 6, the values of D_{SAF} oscillate in a relatively narrow range close to certain values that characterize an out-of-operation cylinder. Table 3 shows the mean values, as well as the maxima, the minima and the standard deviation of D_{SAF} for the analyzed reference range of the speed setpoints.

Table 3 The variability of the differential speed area factor values with respect to the location of combustion loss

Cylinder misfire	1	2	3	4	5	6	7	8
Minimum	9,109	2,451	16,334	8,062	1,000	2,383	3,686	6,562
Maximum	21,712	12,243	27,546	19,128	17,126	21,558	16,258	20,595
Mean	15,737	6,780	22,809	14,394	7,911	9,071	10,299	13,548
Std. dev.	4,029	3,897	3,900	4,231	7,282	6,708	4,417	4,855

Source: authors

Therefore, the differential speed area factor can be used as a tool to locate combustion disturbances (the number of the misfiring cylinder) in addition to the previously presented indicators identifying a combustion problem in the whole engine (without specifying the location of the fault). However, D_{SAF} must first be determined for potential engine fault conditions, and then it can be applied to a given engine.

CONCLUSION

The quantitative indicators presented in this paper for evaluating an engine's instantaneous speed variability, which can be used in the process of evaluating the technical condition of an engine. In particular, the variation in the maximum speed over an engine's complete operating cycle and the uniformity of its speed may serve as a measure of the engine's functionality with respect to the quality of the combustion process occurring in the cylinders. In addition, the differential speed area factor can be used as an additional indicator that can be used to locate a misfiring cylinder.

All these indicators are supplementary to the SpeedMA algorithm presented in the authors' previous paper. Using several tools simultaneously to locate a misfiring cylinder can increase the accuracy of the diagnosis. As a result, the authors expect that their further work will focus on the development of the SpeedMA algorithm by integrating the quantitative indicators that have been presented in this article with the system that was previously developed. Subsequently, the aforementioned indicators will be calculated by the software which analyses the measurements of the engine's instantaneous speed.

This solution has the potential for both commercialization and further development and is therefore protected by two patent applications, no. P.427649 (Polish) and no. 19460053.2 (European).

ACKNOWLEDGEMENTS

This research and publication were co-funded by the Ministry of Science and Higher Education of Poland from Grant 1/S/KPBMiM/20. All product names, trademarks and registered trademarks are property of their respective owners, and they were used in this paper for identification purposes only based on cited resources.

REFERENCES

- Bejger, A., Chybowski, L. and Gawdzińska, K. (2018) 'Utilising elastic waves of acoustic emission to assess the condition of spray nozzles in a marine diesel engine', *Journal of Marine Engineering and Technology*. doi: 10.1080/20464177.2018.1492361.
- Bejger, A. and Drzewieniecki, J. B. (2019) 'The Use of Acoustic Emission to Diagnosis of Fuel Injection Pumps of Marine Diesel Engines', *Energies*, 12(24), p. 4661. doi: 10.3390/en12244661.
- Bejger, A. and Drzewieniecki, J. B. (2020) 'A New Method of Identifying the Limit Condition of Injection Pump Wear in Self-Ignition Engines', *Energies*, 13(7), p. 1601. doi: 10.3390/en13071601.
- Bejger, A. and Piasecki, T. (2020) 'The Use of Acoustic Emission Elastic Waves for Diagnosing High Pressure Mud Pumps Used on Drilling Rigs', *Energies*, 13(5), p. 1138. doi: 10.3390/en13051138.
- Biočanin, S. and Biočanin, M. (2017) 'Measurement crankshaft angular speed of an OM403 engine', *Serbian Journal of Electrical Engineering*, 14(2), pp. 257-275. doi: 10.2298/SJEE1702257B.
- Bonisławski, M. *et al.* (2019) 'A Novel Telemetry System for Real Time, Ship Main Propulsion Power Measurement', *Sensors*, 19(21), p. 4771. doi: 10.3390/s19214771.

- Borkowski, T. Kowalak, P. Myśków, J. (2012) 'Vessel main propulsion engine performance evaluation', *Journal of KONES*, 19(2), pp. 53-60.
- Bueno, A. V., Velásquez, J. A. and Milanez, L. F. (2009) 'A new engine indicating measurement procedure for combustion heat release analysis', *Applied Thermal Engineering*, 29(8-9), pp. 1657-1675. doi: 10.1016/j.applthermaleng.2008.07.023.
- Caputo, D. C. *et al.* (2018) 'Processing of internal combustion engine test data using the indicated cycle provided model', *Transportation Research Procedia*, 33, pp. 20–27. doi: 10.1016/j.trpro.2018.10.071.
- Chybowski, L. (2018) 'Use of Triz SU-Field Models in the Process of Improving the Injector of an Internal Combustion Engine', *Multidisciplinary Aspects of Production Engineering*, 1(1), pp. 257-268. doi: 10.2478/mape-2018-0033.
- Chybowski, L. (2019) *Diagnozowanie silników okrętowych z zapłonem samoczynnym w oparciu o analizę procesów wtrysku i spalania paliwa*. Szczecin: Maritime University of Szczecin Press.
- Chybowski, L. *et al.* (2020) 'Evaluation of Model-Based Control of Reaction Forces at the Supports of Large-Size Crankshafts', *Sensors*, 20(9), p. 2654. doi: 10.3390/s20092654.
- Chybowski, L., Gawdzińska, K. and Laskowski, R. (2019) 'Assessing the Unreliability of Systems during the Early Operation Period of a Ship - A Case Study', *Journal of Marine Science and Engineering*, 7(7), pp. 213:1-12. doi: 10.3390/jmse7070213.
- Chybowski, L., Gawdzińska, K. and Souchkov, V. (2018) 'Applying the Anticipatory Failure Determination at a Very Early Stage of a System'S Development: Overview and Case Study', *Multidisciplinary Aspects of Production Engineering*, 1(1), pp. 205–215. doi: 10.2478/mape-2018-0027.
- Chybowski, L. and Kazienko, D. (2019) 'The Development of an Explosion Protection System in the Starting Air Manifold of a High Power Engine', *System Safety: Human - Technical Facility - Environment*, 1(1), pp. 26-34. doi: 10.2478/czoto-2019-0004.
- Dereszewski, M. (2016) 'Monitoring of torsional vibration of a crankshaft by instantaneous angular speed observations', *Journal of KONES Powertrain and Transport*, 23(1), pp. 99-106.
- Desbazeille, M. *et al.* (2010) 'Model-based diagnosis of large diesel engines based on angular speed variations of the crankshaft', *Mechanical Systems and Signal Processing*, 24(5), pp. 1529–1541. doi: 10.1016/j.ymssp.2009.12.004.
- Dunaj, P., Dolata, M. and Berczyński, S. (2019) 'Model Order Reduction Adapted to Steel Beams Filled with a Composite Material', in *Information Systems Architecture and Technology: Proceedings of 39th International Conference on Information Systems Architecture and Technology – ISAT 2018*. Springer, Cham, pp. 3-13. doi: 10.1007/978-3-319-99996-8_1.
- Dunaj, P., Marchelek, K. and Chodźko, M. (2019) 'Application of the finite element method in the milling process stability diagnosis', *Journal of Theoretical and Applied Mechanics*, 57(2), pp. 353–367. doi: 10.15632/jtam-pl/104589.
- Kazienko, D. (2019) 'The analysis of class survey methods and their impact on the reliability of marine power plants', *55 Scientific Journals of the Maritime University of Szczecin*, no. 55 / 2018, 55(2018-09–27), pp. 34-43. doi: 10.17402/299.
- Kazienko, D. and Chybowski, L. (2020) 'Instantaneous Rotational Speed Algorithm for Locating Malfunctions in Marine Diesel Engines', *Energies*, 13(6), pp. 1396:1-32. doi: 10.3390/en13061396.
- Kluj, S. (2000) *Diagnostyka urządzeń okrętowych*.
- Korczewski, Z. (2015) 'Exhaust gas temperature measurements in diagnostics of turbocharged marine internal combustion engines. Part I. Standard measurements', *Polish Maritime Research*, 1(85), pp. 47-54. doi: 10.1515/pomr-2015-0007.

- Krystosik-Gromadzińska, A. (2019) 'Affordable hybrid thermography for merchant vessel engine room fire safety', *Scientific Journals of the Maritime University of Szczecin, Zeszyty Naukowe Akademii Morskiej w Szczecinie*, 57(129), pp. 21-26. doi: 10.17402/322.
- Li, Z. *et al.* (2012) 'Intelligent fault diagnosis method for marine diesel engines using instantaneous angular speed', *Journal of Mechanical Science and Technology*, 26(8), pp. 2413–2423. doi: 10.1007/s12206-012-0621-2.
- Margaronis, I. E. (1992) 'The torsional vibrations of marine Diesel engines under fault operation of its cylinders', *Forschung im Ingenieurwesen*, 58(1-2), pp. 13-25. doi: 10.1007/BF02561188.
- Nozdrzykowski, K. (2005) 'Comparative assessment of crankshaft strain measurement methods', in *Proc. of 5th International Conference Measurement 2005*. Smolenice, Slovakia, pp. 425-428.
- Nozdrzykowski, K. (2016) 'Force analysis and simulation - experimental research on the measurement of cylindrical surface', *Zeszyty Naukowe Akademii Morskiej w Szczecinie, Scientific Journals of the Maritime University of Szczecin*, 48(120), pp. 37-42.
- Nozdrzykowski, K. and Bejger, A. (2013) 'Aspects of using correlation calculus in comparative measurements of geometric deviations and shape profiles of main crankshaft bearing journals', *Zeszyty Naukowe Akademii Morskiej w Szczecinie, Scientific Journals of the Maritime University of Szczecin*, 35(107), pp. 114-117.
- Nozdrzykowski, K., Chybowski, L. and Dorobczyński, L. (2020) 'Model-Based Estimation of the Reaction Forces in an Elastic System Supporting Large-Size Crankshafts During Measurements of their Geometric Quantities', *Measurement*, 155, p. 107543. doi: j.measurement.2020.107543.
- Piasecki, T. *et al.* (2017) 'Preparation of the Cargo System for LNG Discharge from a Membrane Steam Turbine LNG Vessel at an Offshore LNG Terminal', *Rynek Energii*, 2(129), pp. 95-99.
- Quan, W., Wei, J., Zhao, YW., Sun, LH., Bianl, X. (2011) 'Development of an Automatic Optical Measurement System for Engine Crankshaft.', in *International Conference on Computational Science and Applications*, pp. 68-75.
- Tagliatalata, F. *et al.* (2013) 'Determination of combustion parameters using engine crankshaft speed', *Mechanical Systems and Signal Processing*, 38(2), pp. 628-633. doi: 10.1016/j.ymssp.2012.12.009.
- Ulewicz, R. *et al.* (2019) 'The investigation of the fatigue failure of passenger carriage draw-hook', *Engineering Failure Analysis*, 104, pp. 609-616. doi: 10.1016/j.engfailanal.2019.06.036.
- Ulewicz, R. and Mazur, M. (2013) 'Fatigue Testing Structural Steel as a Factor of Safety of Technical Facilities Maintenance', *Production Engineering Archives*, 1/1, pp. 32–34. doi: 10.30657/pea.2013.01.10.
- VEB SKL (1960) *Buckau-Wolf R8VD-136 Engine Passport. No. 28878*. Magdeburg.
- Wang, T. *et al.* (2019) 'Instantaneous Rotational Speed Measurement Using Image Correlation and Periodicity Determination Algorithms', *IEEE Transactions on Instrumentation and Measurement*, pp. 1-1. doi: 10.1109/TIM.2019.2932154.
- Yang, J. *et al.* (2001) 'Fault Detection in a Diesel Engine by Analysing the Instantaneous Angular Speed', *Mechanical Systems and Signal Processing*, 15(3), pp. 549–564. doi: 10.1006/mssp.2000.1344.

Abstract: A graph of the changes in an engine's operating speed can be used to assess the quality of the combustion in its cylinders. In this paper, the authors carried out tests on a Buckau-Wolf R8VD-136 ship engine, which was directly driving the propeller. This engine is owned by the Laboratory of Marine Engine Rooms at the Maritime University of Szczecin. For standard rotational speeds ranging from 200 to 280 rpm, with increments of 20 rpm, the authors measured the changes in the instantaneous speed for the engine's normal operating conditions (reference graphs) as well as with one of the cylinders being out of operation. A no-combustion situation was successively introduced into each cylinder for each preset rotational speed. The obtained graphs of the instantaneous speed were then used to determine certain quantitative indicators, which the authors believe can provide information about the technical condition of the engine. The analysis concerned the averaged graphs of the speed under the conditions set for five consecutive engine operating cycles. The indicators that were calculated included the maximum difference in the speed over the engine's full operating cycle, the uniformity of the engine speed and the differential speed area factor, the latter a term that has been proposed by the authors. The values of the individual indicators that were obtained from the reference graphs and the graphs with no combustion in one of the cylinders were compared. All indicators are sensitive to cylinder misfire. Conclusions were then drawn on the usefulness of these indicators in assessing the condition of an engine.

Keywords: internal combustion engine, instantaneous speed measurement, cylinder misfire, quantitative indicators, condition monitoring